Preprint
UCRL-JC-142094

Renewable Liquid Optics with Magneto-electrostatic Control

D. Ryutov and A. Toor

This article was submitted to
The International Society for Optical Engineering International Symposium on Optical Science and Technology
San Diego, CA
July 29 - August 3, 2001

June 25, 2001

U.S. Department of Energy
Lawrence Livermore National Laboratory

Approved for public release; further dissemination unlimited

DISCLAIMER

This document was prepared as an account of work sponsored by an agency of the United States Government. Neither the United States Government nor the University of California nor any of their employees, makes any warranty, express or implied, or assumes any legal liability or responsibility for the accuracy, completeness, or usefulness of any information, apparatus, product, or process disclosed, or represents that its use would not infringe privately owned rights. Reference herein to any specific commercial product, process, or service by trade name, trademark, manufacturer, or otherwise, does not necessarily constitute or imply its endorsement, recommendation, or favoring by the United States Government or the University of California. The views and opinions of authors expressed herein do not necessarily state or reflect those of the United States Government or the University of California, and shall not be used for advertising or product endorsement purposes.

This is a preprint of a paper intended for publication in a journal or proceedings. Since changes may be made before publication, this preprint is made available with the understanding that it will not be cited or reproduced without the permission of the author.

This report has been reproduced directly from the best available copy.

Available electronically at http://www.doc.gov/bridge

Available for a processing fee to U.S. Department of Energy
And its contractors in paper from
U.S. Department of Energy
Office of Scientific and Technical Information
P.O. Box 62
Oak Ridge, TN 37831-0062
Telephone: (865) 576-8401
Facsimile: (865) 576-5728
E-mail: reports@adonis.osti.gov

Available for the sale to the public from
U.S. Department of Commerce
National Technical Information Service
5285 Port Royal Road
Springfield, VA 22161
Telephone: (800) 553-6847
Facsimile: (703) 605-6900
E-mail: orders@ntis.fedworld.gov
Online ordering: http://www.ntis.gov/ordering.htm

OR

Lawrence Livermore National Laboratory
Technical Information Department's Digital Library
http://www.llnl.gov/tid/Library.html

Renewable liquid optics with magneto-electrostatic control

D. Ryutov, A. Toor

Lawrence Livermore National Laboratory, Livermore, CA 94551

Abstract

We suggest a new class of high-flux renewable optics, in particular, for the use at the X-ray free electron laser, LCLS, which is under discussion now. The size of optical elements we have in mind is from a fraction of a square centimeter to a few square centimeters. We suggest that working fluid be pressed through a porous substrate (made, e.g., of fused capillaries) to form a film, a few tens to a hundred microns thick. After the passage of an intense laser pulse, the liquid film is sucked back through the substrate by a reversed motion of the piston, and formed anew before the next pulse. The working surface of the film is made flat by capillary forces. We discuss the role of viscous, gravitational, and capillary forces in the dynamics of the film and show that the properly made film can be arbitrarily oriented with respect to the gravitational force. This makes the proposed optics very flexible. We discuss effects of vibrations of the supporting structures on the quality of optical elements. Limitations on the radiation intensity are formulated. We show how the shape of the film surface can be controlled by electrostatic and magnetic forces, allowing one to make parabolic mirrors and reflecting diffraction gratings.

1. Introduction

We propose a new approach to high power-loads on optics and adaptive optics based on the use of liquid optical elements (planar and shaped mirrors, liquid diffraction gratings, and zone plates). The use of liquid optical elements, by itself, is not a new concept. One can cite studies of large-area (many square meters) planar liquid mirrors for laser power plants [1], development of rotating 2.5-m diameter parabolic mirrors for telescopes [2] (see also Ref. 3 for an earlier version of 1.5-m diameter mirror), quasistatic liquid mirrors controlled by $\mathbf{j}\times\mathbf{B}$ forces [4,5], and optical elements made of "ferromagnetic fluids" [6,7].

What we are proposing is entirely different. We propose a new class of centimeter-size renewable optical elements consisting in most cases of thin liquid films over porous substrates, which can be used in rep-rate mode. The principal features associated with these optics are: 1) between two successive pulses the optical elements can be created anew; 2) the film thickness is in the range from a few microns to a hundred of microns and the film's behavior is strongly affected by capillary forces; 3) our optical elements, in most cases, can be arbitrarily oriented with respect to the gravitational force; 4) we use electrostatic and capillary forces to control the shape of the surface of the film.

To designate this new class of optics we will use the acronym "CAMEL" ("CApillary-Magneto-ELectrostatic"). Although in most cases we consider optical elements for short-pulse rep-rate sources, our results describing the magneto-electrostatic control of the shape of the surface have broader applicability and can be used in conjunction with development of low-fluence long-lasting optics (e.g., adaptive optics).

The word "capillary" is used in this paper in two senses. First, we use it as a noun, to designate a thin channel in a solid material. Second, following a long tradition, e.g. [8,9], we use it as an adjective, to designate short-wavelength perturbations on the free surface of the fluid ("capillary waves"). The restoring force for this type of waves is provided by surface tension sometimes called a "capillary force," whence the "capillary waves."

We believe the CAMEL optics provide qualitatively new and important features that will prove to become the enabling technology for a broad variety of applications. many of which are difficult for us to foresee at this time. In the near-term, most important CAMEL optics applications will probably be in the area of x-ray optics for ultra-intense x-ray free electron lasers (the needs of the proposed LCLS facility [10] initially stimulated us to consider pulse-to-pulse renewable capillary diffraction gratings and gave rise to the first steps in the analysis of the CAMEL concept).

A significant advantage of CAMEL optics for rep-rate applications is that the parameters of the optical system can be monitored and changed between two successive pulses at a frequency of ~ 10 Hz.

Although there exists a large variety of liquids suitable for the CAMEL optics, we will make all the numerical estimates only for one liquid, namely mercury, because its parameters are easily available from the literature. In the future work we will assess the perspectives of other liquids. Parameters of the mercury required for our further discussion are listed in Table 1. In cases where we discuss dielectric fluids we assume that their dielectric constant is not much greater than 1, ε-1~1.

In all the general equations we use the CGS system of units; in "practical" estimates we use mixed units specified in each particular case.

TABLE 1. Room temperature parameters for mercury

Density	ρ=13.6 g/cm^3
Kinematic viscosity	ν=1.2·10^{-3} cm^2/s
Electrical conductivity	σ=2·10^{16} s^{-1}
Magnetic diffusivity	D_m=3.5·10^3 cm^2/s
Thermal diffusivity	χ=2.7·10^{-2} cm^2/s
Surface tension	α=500 erg/cm^2
Thermal capacity	c_p=1.9·10^7 erg/cm^{3}K
Sound speed	S=1.5·10^5 cm/s
Volumetric thermal expansion coefficient	β=1.8·10^{-4} K^{-1}

2. Properties of capillary waves.

There exist numerous studies on the theory of capillary waves, summarized in Refs. [8, 9] and many others. For the purpose of our study we need, however, a somewhat "non-traditional" slice of this theory, which cannot be found in one single publication. Therefore, we believe that this introductory chapter will be in place here. In all the numerical examples we will consider the mercury.

2.1 Ideal fluid

Consider a layer of a liquid resting on a planar underlying surface (Fig. 1). The dispersion relation for a small-amplitude wave propagating over this surface is [9]:

$$\omega^2 = \left(kg + \frac{\alpha k^3}{\rho} \right) \tanh(kh) \qquad (2.1)$$

The first term in the bracket in Eq. (2.1) describes a contribution of gravity to the restoring force; the second term describes the contribution of surface tension. These two terms become equal to each other at $k=k^*$, where

$$k^* = \sqrt{\frac{g\rho}{\alpha}} \qquad (2.2)$$

For mercury, this critical wave number is $k^* \approx 5$ cm^{-1} and corresponds to the wavelength of 1.2 cm.

Fig. 2a depicts dispersion curves for mercury film of various depths; Fig. 2b depicts dispersion relation presented in the dimensionless form, with ω measured in units of $(h/g)^{1/2}$, and k measured in units of $1/h$ ($\tilde{\omega} = \omega\sqrt{h/g}$, $\tilde{k} = kh$). In these units the dispersion relation (2.1) reads:

$$\tilde{\omega}^2 = \tilde{k}\left[1 + \frac{\tilde{k}^2}{(k^* h)^2} \right] \tanh \tilde{k} \qquad (2.1')$$

For short wavelengths, $kh>1$, the perturbation is localized near the free surface, and decays exponentially with the distance from the surface, with the e-folding length being $1/k$. The dispersion relation for such perturbations reads as:

$$\omega^2 = \left(kg + \frac{\alpha k^3}{\rho} \right) \tag{2.3}$$

For these short waves, parallel and perpendicular (to the surface) displacements of liquid elements are of the same order of magnitude.

Long-wavelength perturbations, with $kh<1$, occupy the whole layer. The parallel to the surface displacements of liquid elements ($\xi_{||}$) are in this case much greater than perpendicular displacements (ξ_z). These displacements are:

$$\xi_z = z\frac{\delta h}{h}\cos(kx-\omega t); \xi_{||} = \frac{\delta h}{kh}\sin(kx-\omega t), \tag{2.4}$$

where δh is the amplitude of the vertical displacement of the surface. The parallel component is independent of z (up to higher-order corrections in the parameter kh). As is clear from Eq.(2.4), $\xi_{||} \sim \delta h/kh >> \delta h$. The dispersion relation for long-wavelength ($kh<1$) perturbations is

$$\omega^2 = \left(kg + \frac{\alpha k^3}{\rho} \right) kh \tag{2.5}$$

The dispersion relation (2.1) describes also gravitational instability of the liquid film turned "upside down" so that the substrate is now at the top. Dispersion relation in this case can be formally obtained from (2.1) by reversing the sign of g,

$$\omega^2 = \left(-kg + \frac{\alpha k^3}{\rho} \right) \tanh(kh) \tag{2.6}$$

Perturbations are stable (ω real) for short-enough wavelengths, $k>k^*$.

Compressibility of the fluid is unimportant, because the phase velocity is typically much smaller than the sound velocity S. Indeed, for the mercury the phase velocity, $\sqrt{\alpha k/\rho}$, becomes formally greater than S only for unrealistically large k, $k>5\cdot 10^8$ cm^{-1}.

2.2 Viscous effects

Viscosity causes damping of stable perturbations. It cannot stabilize unstable perturbations with ($k<k^*$) in the case of inverted geometry but, in some cases, can reduce their growth rate.

In the case of short wavelengths, $kh>1$, the damping rate $\mathrm{Im}\,\omega$ is equal to:

$$\mathrm{Im}\,\omega = -2\nu k^2 \tag{2.7}$$

For long wavelengths, $kh<1$, the damping rate depends on the parameter $\omega\tau$, where τ is a characteristic time for viscous shear flow to propagate over the film thickness h,

$$\tau \equiv \frac{h^2}{\nu} \tag{2.8}$$

For a mercury film with h=25 μm, one has $\tau=5.2\cdot 10^{-3}$ s.

We will need the damping rate only for the case of small $\omega\tau$. In this domain, perturbations become essentially aperiodic, with $\mathrm{Im}\,\omega >> \mathrm{Re}\,\omega$, and

$$\mathrm{Im}\,\omega \approx -\frac{h^3 k^2}{3\nu}\left(g + \frac{\alpha}{\rho}k^2\right) \tag{2.9}$$

(see Ref. [11] and references therein). For the inverted configuration, and wavelengths with $k<k^*$, the system is unstable, with the growth rate being, roughly speaking,

$$\mathrm{Im}\,\omega \approx \frac{h^3 k^2 g}{3\nu} \tag{2.10}$$

3. Creating a planar renewable mirror by pressing a liquid through a porous substrate.

3.1 General approach

Fig. 3 shows a concept of creating a planar renewable mirror with an upside-down orientation. A planar, arbitrarily oriented mirror is a very important element of the optical system because it allows one to produce an arbitrary transformation of the light beam with the other liquid optical elements having a "normal" orientation (Fig. 4). The liquid film in Fig. 3 is formed by pressing a working fluid through a porous substrate by a piston. Before the gravitational instability has developed, the piston sucks the liquid back, and the cycle repeats. To be specific, we assume that the substrate is made of fused capillaries of the same radius r_{cap}. Other porous substrates are conceivable, but we leave their analysis for the further work. In real life, it may be more convenient to push and pull the liquid not by a piston, but by a flexible membrane driven by actuators situated behind it. In our conceptual discussion, we, however, will talk solely about a piston.

We suggest using non-wettable substrate. This will probably allow a complete removal of the liquid from the outer side of the system during the "in" move of the piston. For the wettable substrate, one can expect that droplets will stick to the areas between the holes of the capillaries. A mechanical barrier (a rim) in Fig. 3 of the height approximately equal to the film thickness could be used to prevent the film from spreading laterally. A wettable substrate (with non-wettable rim) is also conceivable. It is difficult to make the final choice without some experimentation.

Let's consider one cycle of the motion of the piston, starting on from the position where the liquid film is present on the outer surface of the porous substrate. The piston begins moving away from the substrate and, by the end of a half-cycle, "sucks" the liquid out of the capillaries into the volume behind the substrate (Fig. 3). On the reverse motion, the piston presses the fluid through the capillaries and creates a liquid film with a high-quality reflecting surface. In other words, we assume that the stroke of the piston is equal to the thickness b of the substrate (plus the film thickness, which is usually negligible compared to b). In principle, it may suffice to have a stroke as small as a few thicknesses (h) of the liquid film. We, however, will discuss a more difficult in realization case of a larger stroke. This larger stroke may be necessary if one wants to extract all the working fluid from the capillaries during every cycle. A continuing lateral flow of the working fluid through a plenum behind the substrate (1 in Fig. 3) could then be organized to gradually refresh it. A cleaning system could be introduced in this contour.

3.2 Deformations of the substrate

Obviously, to provide a smoothest possible surface of the mirror, the radius of capillaries, r_{cap}, should be made as small as possible. On the other hand, the pressure required to push the fluid through capillaries, Δp, increases as $1/r_{cap}$:

$$\Delta p = \frac{2\alpha}{r_{cap}} \ . \qquad (3.1)$$

For wettable materials one would have to apply a negative Δp to suck the liquid out of the capillary. When making the estimate (3.1), we considered perfectly non-wettable or perfectly wettable material, with the contact angle being either 180^o or 0^o. The pressure Δp applied to the substrate causes its deformation, which we will evaluate in this sub-section.

For the mercury,

$$\Delta p(atm) \approx \frac{10}{r_{cap}(\mu m)}. \qquad (3.2)$$

We do not want to make Δp too large, to avoid too strong deformation of the substrate; this pushes us in the direction of the larger radii r_{cap}. For the numerical example we choose r_{cap} =5 μm. According to Eq. (3.1), this corresponds to the pressure of 2 atm.

The maximum displacement Δb of the substrate occurs in its center. Displacement amplitude is [12]:

$$\Delta b = \frac{3(1-\mu^2)R^4 \Delta p}{16 b^3 E}, \qquad (3.3)$$

where R is the mirror radius, E is the Young's modulus, and μ is the Poisson coefficient of the substrate. To make an upper-bound estimate of Δb, we assume that E is 10 times less than the Young's modulus for the steel, i.e., we take $E=2\cdot 10^{10}$ n/m^2. With regard to μ, we take a value of 0.3, typical for many materials. Assuming, as before, that R=0.5 cm, and b=0.1 cm, we find that $\Delta b \sim 1\ \mu m$, the value that looks acceptable.

The characteristic frequency of the lowest mode of elastic vibrations of the substrate is

$$\omega \sim \sqrt{\frac{b^2 E}{R^4 \rho}}, \qquad (3.4)$$

where ρ is the substrate density. Taking ρ=2 g/cm^3, and the other parameters as before, one finds that the resonant frequency is ~10^5 s^{-1}, orders of magnitude higher than the frequency of the piston motion. This justifies using a steady-state approximation in evaluating Δb.

Rough estimates of displacement and of the lowest eigenfrequency for a rectangular membrane can be obtained by replacing R in Eqs. (3.3) and (3.4) by $\left(2L_1^{-2} + 2L_2^{-2}\right)^{-1/2}$, where L_1 and L_2 are the lengths of the sides of the rectangle.

An additional force on the membrane will appear because of the viscous friction of the working fluid against the walls of the capillaries. We assume that liquid inside capillaries performs a vertical sinusoidal motion with the period t_{piston} and the amplitude $b/2$ (the distance between the upper and the lower position of the surface is then equal to the thickness of the substrate). This motion is driven by the piston. The amplitude of the viscous friction force between the walls and the liquid can be estimated as $2\pi^2 b^2 \nu\rho / t_{piston}$. The number of capillaries per unit surface area of the substrate is $\eta / \pi r_{cap}^2$, where η (~1) is a filling factor by which we mean the ratio of the area occupied by the holes to the total area of the substrate. Multiplying the two quantities, one finds additional pressure required to press the fluid through capillaries:

$$\Delta p_{visc} = \frac{2\pi\eta b^2 \nu\rho}{r_{cap}^2 t_{pist}}. \qquad (3.5)$$

For mercury, and η=0.5, r_{cap}=5 μm, b= 1mm, and t_{pist}=0.1s one finds that Δp_{visc}~0.035 atm and can be neglected compared to the pressure perturbation (3.2).

Two caveats are in order here. First, the real motion of the piston will probably be not a pure sinusoid. It might be worth adding a "plateau" on the dependence of the piston position vs time around the point where the thickness of the fluid film has reached a desired value. This would eliminate any unnecessary motions that could distort the surface of the film around the time when the optical pulse arrives. For the period of 0.1 s this plateau could probably be 0.02 s long. However, the presence of this relatively short plateau will have no significant effect on the estimate of the force (3.5). The second caveat is related to the fact that, when making estimate (3.5), we have implicitly assumed that the fluid flow in the capillary is a pure Poiseuille flow. In fact, the presence of the free surface of the fluid leads to a more complex 2D flow near the surface. We neglect this subtlety in our estimates because of a very large b/r_{cap} ratio.

3.3 The waviness of the reflecting surface.

The substrate is made of many capillaries closely packed together. As we assume that the walls of the capillaries have a thickness of the order of r_{cap} (η~1), the spatial scale of the surface structures can be estimated as r_{cap}. When the fluid is pressed through the capillaries, its surface gets rippled at this scale or, in other words, the ripples have a characteristic wave number k~$1/r_{cap}$. These ripples experience a rapid viscous damping described by Eq. (2.7). For mercury and r_{cap}= 5 μm one has Imω~10^4 s^{-1}; in other words, these perturbations damp away during a small fraction of the period. Generally speaking, initial perturbations will have a broad spectrum where also longer wavelengths will be present. Specific details of the spectrum will be determined by possible larger-scale correlations between positions of individual capillaries. These correlations will depend on the manufacturing process and are unknown to us at this stage. One can only say that even perturbations with spatial scales ~$10r_{cap}$ decay relatively quickly, within ~10^{-2} s.

A special class is formed by long-wave perturbations with $k<k^*$, which are unstable for the upside-down orientation (See Sec. 2.1). The finite radius of the mirror limits wave number of perturbations from below, by the value approximately equal to

$$k_{min}=1.5/R \qquad (3.6)$$

(the exact numerical coefficient depends on the boundary conditions on the rim). For mercury, and R=0.5 cm, the unstable mode is indeed present ($k_{min}<k^*$). However, it grows very slowly because of the viscous effects. Indeed, Eq. (2.10) shows that for a 25 μm thick mercury film, and k=3 cm^{-1}, the growth rate is $6\cdot10^{-2}$ s^{-1}. The corresponding e-folding time is 15s, much longer than the period of the piston motion. For a rectangular mirror with the lengths of the sides equal to L_1 and L_2, under the assumption that displacement is zero on the boundaries, the minimum wave number is

$$k_{\min} = \pi\sqrt{\frac{1}{L_1^2}+\frac{1}{L_2^2}} \qquad (3.7)$$

Although the instability by itself is not a big problem (because of its small growth rate), the absence of the restoring force for the perturbations with $k<k^*$ means that at the large scales the film must be perfect during the whole time of its creation, with tilts or bumps with a scale $k<k^*$ being inadmissible. This means that the properties of the porous substrate must be uniform to a high level of precision at these scales.

As the long-wavelength instability is so slow, it is not a limiting factor in the increase of the size of the mirror. The uniformity of the substrate at larger scales may pose more serious problems.

Conversely, if one wants to have a mirror that would be stable for all perturbations, and whose surface would experience restoring forces bringing the surface to an equilibrium shape (thereby relaxing requirements to the quality of the substrate), one might want to reduce its radius R to the values below, roughly speaking, $1.5/k^*$ (3 mm for mercury). The problem is that the equilibrium shape for a small mirror will not be planar, but will be a meniscus. One may apply a correction technique based on the use of electrostatic forces (see Sec. 4) to produce a planar part around the center of the mirror (Fig. 5). Although we haven't made yet analysis of the other candidate fluids, it is possible that there exists fluids with k^* smaller than in case of mercury. This would allow one to increase the mirror radius beyond 3 mm. We have yet to study whether electrostatic forces introduce new instabilities.

There exists a general question of what is the minimum possible level of deviations of the mirror surface from planarity in the stable domain. This minimum possible level is determined by thermal fluctuations. The spectral energy density W_k of thermal fluctuations is defined by the equation:

$$dW = W_{\mathbf{k}} dk_x dk_y \tag{3.8}$$

where dW is the energy of surface oscillations in the interval of wave numbers dk_x, dk_y per unit surface area of the plane. For thermal fluctuations, one has

$$W_{\mathbf{k}} = \frac{T}{(2\pi)^2} \tag{3.9}$$

(the Rayleigh-Jeans distribution, with T being the temperature of the film). On the other hand, W_k is related to the spectral density of surface displacements $(\xi^2)_{\mathbf{k}}$ via equation:

$$W_{\mathbf{k}} = \frac{\left(\xi^2\right)_{\mathbf{k}} \omega_k^2 \rho}{k} \cdot \frac{\sinh(2kh)}{\cosh(2kh)-1} = \left(\xi^2\right)_{\mathbf{k}} \left(\rho g + \alpha k^2\right) \tag{3.10}$$

(we have used dispersion relation (2.1)). Equations (3.9)-(3.10) then yield the following expression for the contribution $d\xi^2$ of the interval dk_x, dk_y to the mean-square deviation of the surface from the plane:

$$d\xi^2 \equiv \left(\xi^2\right)_k dk_x dk_y = \frac{T}{(2\pi)^2 \left(\rho g + \alpha k^2\right)} \cdot dk_x dk_y \tag{3.11}$$

Remarkably, this result coincides with the previously derived expression for $d\xi^2$ for the fluid of an infinite depth [13]. For capillary waves (i.e., the waves with $k>k^*$, Eq. (2.2)), one obtains:

$$d\xi^2 \equiv \frac{T dk}{2\pi k \alpha} \tag{3.12}$$

We have taken into account that $dk_x dk_y = 2\pi k dk$. The contribution to the surface roughness from the wave numbers whose absolute values lie between k_1 and k_2 is:

$$\xi^2(k_1 < k < k_2) = \frac{T}{2\pi\alpha} \ln\left(\frac{k_2}{k_1}\right) \tag{3.13}$$

The longer wavelengths, $k<k^*$, give smaller contribution. One sees that for a rough estimate of the r.m.s. value for deviations from planarity one can use an equation

$$\sqrt{\left\langle \xi^2 \right\rangle} \approx \sqrt{\frac{5T}{2\pi\alpha}} \tag{3.14}$$

where we have replaced the logarithmic factor by its typical numerical value ~ 5. For mercury at the temperature ~$4.5\cdot10^{-14}$ erg (300 ^{0}K), one has $\sqrt{\langle\xi^2\rangle}$~1 Å. This determines the minimum possible surface roughness. As was pointed out in Ref. [13], the actual roughness may be somewhat larger than (3.13) because of the finite size of atoms (or molecules) forming the fluid.

3.4 The role of vibrations.

High-precision optical elements installed on an experimental facility usually experience some level of vibrations originating from external sources. There is an issue of possible misalignment caused by these vibrations. For the optical systems a great experience has been accumulated in dealing with this problem. In this sense, solid elements of the system discussed above (e.g., substrates) do not create any specific new problems. A question may arise, though, on how vibrations could affect liquid surfaces.

Typical frequencies of vibrations, ω_{vibr}, lie in the range below 300 s^{-1}. They are below the eigenfrequencies of the substrate (Eq. (3.4)). We therefore assume that the substrate moves as a perfectly rigid body. This motion can be represented as a superposition of translational motion and tilts.

We first consider translations. We characterize them by a displacement vector $\xi(t)$. The translational acceleration $d^2\xi/dt^2$ can be represented as a sum of the tangential and normal acceleration. The normal acceleration does not change the shape of a planar surface of the mirror. So, we consider tangential acceleration. It causes a fluid flow along the surface of the mirror and leads thereby to tilting of the liquid surface. For relatively low frequencies mentioned above and thin-enough films, the condition $\omega_{vibr}\tau<1$ holds (where τ is defined as in (2.8)), meaning that the tangential velocity is a linear function of the distance from the substrate surface (Couette flow), with the average (over the film thickness) velocity equal to

$$\bar{v} = \frac{\tau\ddot{\xi}_t}{2}, \tag{3.15}$$

where by ξ_t we mean only tangential component of the displacement. This flow causes increase of the depth on one side of the mirror and decrease on the other side. The estimate for the relative displacement Δh of the fluid surface at two opposite sides of the disk then follows,

$$\Delta h \sim \frac{h\omega_{vibr}^2\xi\tau}{R}\min(\omega_{vibr}^{-1}, \Delta t) \tag{3.16}$$

where Δt is a time interval during which thin film exists at the outer surface of the substrate (0.03 s in the example given in Sec. 3.2). We deliberately overestimate Δh by writing ξ instead of ξ_t.

The tilt of the surface of the film relative to the substrate is $\Delta h/R$. In order to be unimportant, it must be less than the tilt of the substrate itself, θ. The latter is related to the displacement by $\theta\sim\xi/L$, where L is the size of the structural element of the facility to which the mirror system is attached, or the wavelength of vibrations in this element, if the latter is shorter. In this way we arrive at the following criterion for unimportance of specifically "fluid" effects in vibrations:

$$\frac{hL\omega_{\text{vibr}}^2\tau}{R^2}\min(\omega_{\text{vibr}}^{-1},\Delta t)<1 \qquad (3.17)$$

As we have already mentioned, for thin-enough films, one has $\omega_{\text{vibr}}\tau<1$. This means that condition (3.17) is certainly satisfied if $hL<R^2$; for our standard set of parameters, R=0.5 cm, h=25 μm, this latter inequality holds if L<100 cm.

The normal component of the acceleration does not affect the planar surface of the liquid film but it may affect the curved surface of the type we discuss in the next section. We will not present here the corresponding simple analysis. It is also worth noting that tilts of the substrate cause smaller tilt of the liquid surface relative to substrate than tangential accelerations we have just discussed. We leave further details for the future reports.

3.5 Maximum intensity of the laser pulse.

There are two limitations on the intensity of the laser pulse that can still be handled by the proposed system without damaging its permanent components. The first is decrease of the reflectivity during the laser pulse itself (because of, e.g., bringing the surface to a boil temperature during the pulse). The second is possible damage to the substrate by mechanical and thermal perturbations initially produced near the surface of the liquid and then propagating towards the substrate. The first constraint is not specific to our concept. There exist numerous studies of that issue. We therefore discuss only the second constraint, limiting ourselves to a qualitative discussion. We consider a 1-dimensional problem, assuming that the spot size on the surface of the film is greater than the film thickness.

There are two characteristic times important in the problem, the sound propagation time through the film, h/S (where S is the sound velocity), and the time of a thermal diffusion, h^2/χ (where χ is thermal diffusivity). For a 25 μm-thick mercury film, the acoustic time is ~ $2\cdot10^{-8}$ s, and the thermal conduction time is $2\cdot10^{-4}$ s.

The characteristic pulse-width of the x-ray pulse in the LCLS project is in the range of 200-300 fs. As the laser pulse is shorter than the acoustic time, the pressure perturbation created near the surface, propagates as an acoustic pulse (which may become a shock wave, if the amplitude is large enough). The energy deposition occurs at a depth Δh ~ 0.3 μm in mercury (this is determined by photo-absorption of x rays and subsequent energy transport by keV-range electrons). The liquid within this layer is heated up to some temperature ΔT virtually instantaneously (compared both to the sound propagation time and the heat conduction time over Δh). The resulting pressure perturbation Δp then drives an acoustic pulse propagating towards the substrate. It may form a weak shock by the familiar overtaking process [9]. The shock is formed if the condition

$$\Delta p > \rho S^2 \frac{\Delta h}{h} \qquad (3.18)$$

holds. By noting that the pressure perturbation in the isochoric heating can be evaluated as

$$\Delta p_0 \sim \rho S^2 \beta \Delta T \qquad (3.19)$$

(where β is volumetric thermal expansion coefficient), one finds that the shock is formed if

$$\Delta T > \frac{\Delta h}{\beta h} \qquad (3.20)$$

For mercury in the aforementioned example, the shock is formed if ΔT>50 K. This corresponds to the deposited energy $C_p\Delta h\Delta T$>3 mJ/cm^2.

If the shock is indeed formed, it weakens during its propagation through the film [9]; the pressure jump at the distance h from the surface decreases to $\Delta p \sim \sqrt{\rho S \Delta p_0 \Delta h / h} < \Delta p_0$. For the energy deposition in the range of the critical value of 3 mJ/cm^2, the expected pressure amplitude will be in the range of 3 Kbar, somewhat below the yield strength of good structural materials. Of some concern may be behavior of the shock near the edges of the capillaries where the energy concentration may occur as a result of reverberations. To answer this question, experiments or 3D numerical simulations may be needed.

For longer-pulse, higher energy-per-pulse lasers, the favorable regimes of operation are those where the pulse width is larger than the sound propagation time h/S, so that thermal stresses in the heated surface layers increase adiabatically slowly, and do not lead to shock formation. They just cause a quasi-equilibrium thermal expansion of the heated layer, with only small pressure increase in the bulk of the film. If the pulse is shorter than h/S, it is at least desirable to make it longer than $\Delta h/S$. The pressure perturbation in the pressure pulse that will be propagating towards the substrate will then be much less than Eq. (3.19).

4. Electrostatically controlled mirrors

4.1 Mirror focal length

Another CAMEL configuration would be a parabolic mirror in a thin layer of a liquid, with a substrate being a flat conducting plate. A ring electrode of a radius R will be situated at some distance ($\sim R$) over the surface. Electric field will distort the surface of the fluid, with the region near the axis forming a parabolic mirror (Fig. 6). If a thin ring is situated at a distance a from the surface of the plate, the electric field at the planar surface of the conducting fluid (kept at the ground potential) is determined by the equation

$$E_z(r) = \frac{2URa}{\Lambda} \int_0^{\pi} \frac{d\varphi}{\left(a^2 + R^2 - 2Rr\cos\varphi + r^2\right)^{3/2}} \tag{4.1}$$

where U is the ring potential, and Λ is a logarithmic factor depending on the (small) thickness d of the ring {$\Lambda \approx \ln[2\min(a, R)/d]$}; r is the distance from the axis of symmetry. Under the action of the ponderomotive force, the surface becomes perturbed. However, these perturbations are small (at least for the mirrors with the focal distance much greater than the mirror radius). We will neglect these small corrections when evaluating E_z. If there is a need to refresh the fluid between the two subsequent pulses, one can use a conducting, porous substrate.

For large-focal-length mirrors deviations of the surface from planarity are small, $\Delta h << R$, and one can use the linear equation to find Δh :

$$\frac{\alpha}{r}\frac{d}{dr} r \frac{d\Delta h}{dr} = \rho g \Delta h - \frac{E_z^2}{8\pi} \tag{4.2}$$

We will study its solution near the axis, at small r. In this zone the ponderomotive force can be presented as an expansion:

$$\frac{E_z^2}{8\pi} = \frac{\pi (Ua)^2}{2\Lambda^2 \left(a^2 + R^2\right)^3} \left[1 + C_1 \left(\frac{r}{R}\right)^2 + C_2 \left(\frac{r}{R}\right)^4 + \ldots\right] \tag{4.3}$$

We limit ourselves to the first three members. One has:

$$C_1 = \frac{3R^2\left(3R^2 - 2a^2\right)}{2\left(a^2 + R^2\right)^2}; C_2 = \frac{3R^4\left(4a^4 - 17a^2R^2 - \frac{329}{64}R^4\right)}{2\left(a^2 + R^2\right)^4} \tag{4.4}$$

If we are interested in not-too-small mirrors, with the size exceeding $1/k^*$, one can neglect capillary forces and set the left hand side (l.h.s.) of Eq. (4.2) to zero. Then one obtains the following expression for the function $\Delta h(r)$:

$$\Delta h(r) = \frac{\pi(Ua)^2}{2\rho g\Lambda^2\left(a^2 + R^2\right)^3}\left[1 + C_1\left(\frac{r}{R}\right)^2 + C_2\left(\frac{r}{R}\right)^4 + ...\right] \tag{4.5}$$

If corrections related to the finite value of the capillary forces are required, one can find them by substituting this solution to the l.h.s. of Eq. (4.2). The ideal parabolic mirror corresponds to all the terms beyond r^2 being equal to zero. The focal length in the paraxial domain, where the third and higher-order terms in the R.H.S. of (4.5) can be neglected, is

$$F = \frac{\rho g\Lambda^2\left(a^2 + R^2\right)^5}{3\pi(Ua)^2\left(3R^2 - 2a^2\right)} \tag{4.6}$$

At given voltage U and radius R of the ring, the focal length varies as a function of the distance a between the ring and the surface. At small a, the surface near the axis is almost flat, and the focal length is infinite. It reaches a minimum at the distance $a \approx 0.45R$. At the further increase of a, the surface near the axis again becomes flat (at $a=1.22R$), and then becomes convex, giving rise to a defocusing mirror. The minimum focal length for the defocusing mirror is attained at $a \approx 1.57R$. Finally, at even larger a's, the surface again flattens.

At the distance $a \approx 0.45R$ corresponding to the minimum focal length, one has

$$F = F_0 \equiv \frac{0.51\rho g\Lambda^2 R^6}{U^2} \tag{4.7}$$

Eq. (4.7) shows that, with mercury as the working fluid, creating a mirror with a focal length of 50 cm by a ring of the radius R=0.5 cm requires a modest voltage ~ 1.5 kV (we assumed Λ=3). With this voltage, the maximum value of Δh (which is reached just under the ring, at $r \approx R$) is approximately 30 μm. This sets the minimum value of the initial thickness of the liquid film, which must be greater than ~ 30 μm.

One advantage of this scheme is that it works not only for conducting but also for dielectric fluid (for the latter, the result analogous to Eq. (4.5) will also depend on the dielectric constant). Another advantage is related to a possibility of using several ring electrodes segmented in the azimuthal direction, each with an independent voltage control. By proper adjustment of the voltages applied to azimuthal segments, on can create an approximately parabolic mirror with an axis tilted with respect to the normal to the surface. This demonstrates one outstanding feature of the CAMEL concept: remote control of the focal length and optical axis of a figured mirror, without introducing any mechanically moving parts.

A relative disadvantage of this scheme is the presence of the electrodes in front of the mirror. This limits the solid angle that can be used for collecting light. For dielectric liquids, however, one can solve this problem by using a ring situated below the liquid film and dielectric substrate, as shown in Fig. 7.

4.2 Characteristic time-scales for changing the shape of the mirror.

Consider a pool of liquid of the thickness $h<<R$. If one wants to vary the focal length and orientation of the optical axis by varying the voltages at different electrodes, one has to evaluate the characteristic time $\tau_{response}$ within which the liquid will redistribute itself over the surface of the substrate and settle down in the new equilibrium. For thin films, viscous forces may be important and could slow down the response time. Basically, this time is equal to the time of viscous damping of surface waves with the wave-number $k\sim 1/R$. For not too thick films, the damping rate is determined by Eq. (2.9), with the lst term neglected (because we assume that $k*R>1$) According to the estimate (2.9), we have

$$\tau_{response} \sim \frac{2\nu R^2}{h^3 g} \tag{4.8}$$

For a mercury mirror with R=0.5 cm and h=30 μm, one finds $\tau_{response}$ ~20 s. According to Eq. (4.8), the response is faster for thicker mirrors. At some point, however, the response time evaluated according to Eq. (4.8) becomes shorter than the viscous time (2.8), and applicability conditions of Eq. (2.9) (or, equivalently, Eq. (4.8)) break down. The maximum thickness at which one can still use Eq. (4.8) can be evaluated from the condition $\tau_{response}\sim\tau$ (with τ as in Eq. (2.8)), which yields:

$$h \sim \left(\frac{2\nu^2 R^2}{g}\right)^{1/5} \tag{4.9}$$

The corresponding response time is

$$\tau_{response} \sim \left(\frac{4R^4}{g^2\nu}\right)^{1/5} \tag{4.10}$$

For the mercury mirror with R=0.5 cm, one has h=150 μm, and the corresponding shortest response time ~0.2 s.

For the film thicker than the one evaluated from Eq. (4.9), the response will be accompanied by excitation of the wave motion of the fluid. One could significantly reduce the amplitude of transient waves by applying the voltage in an "adiabatically slow" fashion. How much one can gain then in terms of the response time, will be analyzed in further reports. Too thick films, on the other hand, may be too vulnerable to vibrations (see Sec. 3.4).

4.3 Liquid dielectric zone plate

By introducing a set of properly spaced rings underneath the surface of the dielectric film, and charging them, one can produce a set of concentric bumps and dips on the surface (Fig. 8), via the action of the ponderomotive force. The width of each bump (dip) should be equal to the width of the corresponding Fresnel zone. This will not be a step-wise zone plate, because transitions between tops and bottoms of the surface structure will be smooth, but it will work in a similar way, yielding a significant amplification of the light intensity in the focal point.

For a normal incidence, the required height of the surface features is $\Delta h\sim\lambda_x/4$, where λ_x is the wavelength of the light. The width of the every zone is much larger: the scale is $\ell\sim(\lambda_x F)^{1/2}$, where F is the focal length. The required electric field strength on the surface of the film is determined by balancing the ponderomotive force, $E^2/8\pi$, against the capillary force, which scales as $\alpha\Delta h/\ell^2$, where α is the capillary constant. When writing the ponderomotive force, we assume that the dielectric constant of the film, ε, is not very large, ~1. Equating the two forces, one obtains the following estimate for the required electric field

strength: $E^2/8\pi \sim \alpha/4F$. Taking as a representative value of the capillary constant α~100 erg/cm^2, and the focal distance F~100 cm, one finds that the required electric field strength is ~ 1 kV/cm. For visible light (λ_x ~0.5 μm) and the focal length 100 cm, the size of the first few Fresnel zones is equal to ~0.7 mm. This sets the scale of the voltages required to create the aforementioned electric field: ΔU~70 V. The thickness of the film should be of order of ℓ/π (in the aforementioned example this is ~ 200 micrometers).

For X rays with the wavelength of 1.5 Å, one has to use grazing incidence optics, with the incidence angle θ (counted from the surface of the plate) being ~ 10 mrad or less (otherwise, the reflectivity becomes prohibitively low). In this case, it is inefficient to use circular zone plate. Instead, one can use a linear zone plate, providing a cylindrical focus. The length of the plate will then be much greater than its width. For small θ, the required amplitude of surface relief becomes $\Delta h \sim \lambda_x/4\theta$ and the width of the zones becomes $\ell \sim (\lambda F)^{1/2}/\theta$. For the focal length of 100 cm and $\theta=10^{-2}$, ℓ is ~ 1 mm, and Δh is ~40 Å. For the film thickness ~ 300 μm, the electric field required to produce this surface relief becomes ~ 100 V/cm, with the voltage between neighboring wires (separated by the distance ~ 1mm) in the range of 10 V. It is assumed that the incident beam is broad enough so that the length of its imprint ias at least a few times greater than ℓ.

5. Capillary diffraction gratings

5.1 Using ferroelectric transducers

It is obvious that the surface of the liquid film, if rippled by a capillary wave, can serve as a reflecting diffraction grating. It looks especially attractive for rep-rate systems with high energy flux, which would require replacement of the grating after every pulse. With the grating created anew on the surface of a liquid film (which is also replaced after every pulse), one can operate at high rep-rates, determined by the time of replacement of the film (up to ~ 100 Hz). The most obvious way of launching a capillary wave is using a transducer (say, a ferroelectric transducer) situated at one side of the film and exciting a capillary wave of a desired wavelength propagating towards the other edge.

Unfortunately, this technique does not work for short-enough grating periods, below a few micrometers for mercury. The problem is that short-wavelength capillary waves damp very rapidly because of the viscous dissipation (Eq. (2.7)). For short wavelengths, one can neglect the contribution of the gravitational force to the dispersion relation (2.3). The group velocity of the capillary wave is then

$$v_{group} = \frac{3}{2}\sqrt{\frac{\alpha k}{\rho}} \tag{5.1}$$

Dividing it by the damping rate Imω (Eq.2.7), one finds the e-folding length ℓ_{abs},

$$\ell_{abs} = \frac{3}{4}\sqrt{\frac{\alpha}{\rho \nu^2 k^3}} \tag{5.2}$$

For the wavelength of 10μm on the surface of mercury, the absorption length is a mere 60 μm, only 6 wavelengths. For shorter wavelengths this number decreases further. Therefore, for a single transducer, it is difficult to create a “capillary grating” of a reasonable length. One could consider a set of phased transducers separated by the distance of, say, $\ell_{abs}/2$. But a long array required to produce a diffraction grid with, say, 10^4 periods would be relatively more expensive than the system we describe below.

5.2 Using the electromagnetic drive

We suggest to generate a standing wave perturbation by **J**×**B** force. Consider an array of thin parallel wires placed on the surface of the dielectric substrate (possibly in precisely machined grooves), with the wires being in electric contact with mercury (Fig. 9). We impose a constant magnetic field of B_0~10 kG strength, oriented along the wires. Such a field can be created by permanent magnets. A sinusoidal voltage will be applied between the neighboring wires and will drive the current in mercury. Interaction of this current with the external magnetic field will excite a capillary wave on the surface of the film. The wavelength will obviously equal to the doubled inter-wire distance. To be specific, we consider the phasing that corresponds to a standing wave (although generation of the traveling wave is also possible). To reduce the requirements to the current density, we choose the frequency of the current to coincide with the frequency of the capillary wave with the desired period (determined by the distances between the neighboring wires). The creation of reflection gratings with 10 μm period will require a voltage frequency in the range of 1 MHz.

We assume that the thickness of the film is not very much larger than *1/k*; otherwise, perturbations produced by the currents flowing near the bottom will be too weakly coupled with surface perturbations. To be specific, we assume that the thickness is

$$h=A/k, \tag{5.3}$$

with the numerical coefficient A being equal 2-3.

The time for the magnetic diffusion over the thickness *h*,

$$\tau_{magn} = \frac{h^2}{2D_m}, \tag{5.4}$$

is quite short. For the mercury and h=5 μm it is less than 1 ns (see Table 1 for D_m); in other words, the current is distributed resistively, and isn't strongly localized near the substrate: it flows over the whole thickness of the liquid film. If the current per unit length of the wire is *J*, then the parallel to the surface component of the current density is $j \sim J/h$. The vertical force acting per unit volume of the film can then be evaluated as

$$f_z \sim \frac{jB_0}{c}, \tag{5.5}$$

where B_0 is the external magnetic field. Consider first the static case, where the inter-wire voltage (and, accordingly, *j*) does not vary with time. This vertical force, integrated over the film thickness, is then balanced by the surface tension, so that

$$f_z h \sim \alpha k^2 \xi_0, \tag{5.6}$$

where ξ_0 is the surface deformation in the static case. From Eqs. (5.5) and (5.6) one finds that

$$\xi_0 \sim \frac{jB_0 h}{\alpha k^2 c} \sim \frac{jB_0 A}{\alpha k^3 c}, \tag{5.7}$$

where we have used Eq. (5.3).

To reduce requirements to the driving current, we will exploit the resonance excitation, in other words, we will adjust the frequency of the current to be equal to the eigenfrequency of the capillary wave with the wavelength determined by the period of the exciting force (two inter-wire distances). For the sinusoidal dependence of the exciting force over the time, one has:

$$\ddot{\xi} + 4\nu k^2 \dot{\xi} + \omega_0^2 \xi = \omega_0^2 \xi_0 \cos \omega t \tag{5.8}$$

The second term describes viscous damping (Eq. (2.7)). If the frequency ω coincides with the resonant frequency ω_0, the amplitude of the surface oscillations can be evaluated as

$$\xi \approx \xi_0 \frac{\omega_0}{\max(4\nu k^2, 1/\Delta t)} \tag{5.9}$$

Here we have taken into account that, in some cases, the duration Δt of the wave-train in the wire array may be shorter than the inverse damping time. In particular, this may be the case when the viscous damping is small.

For the 10 μm wavelength ($k=6.28\cdot10^3$ cm^{-1}) in mercury, one has $\omega_0 \approx 3\cdot10^6$ s^{-1}, and $4\nu k^2 \approx 1.8\cdot10^5$ s^{-1}. Therefore, for a driving pulse duration Δt exceeding 10-20 μs, the amplitude of the surface perturbations will be ~15 times higher than the amplitude of static perturbations ξ_0.

Assume that the wave amplitude is approaching nonlinear state, with $k\xi \sim 0.3$ (or, in other words, peak-to-valley distance equal to 0.1 of the wavelength), meaning that $\xi_0 \sim 0.02/k \sim 3\cdot10^{-6}$ cm. Equation (5.7), with $A=2.5$, and $B_0=10$ kG yields then the following expression for the required current density: $j \sim 10^{14}$ CGS~30 kA/cm^2. The resulting magnetic field perturbation is $\Delta B \sim 10$ G. The forces acting upon the fluid can be evaluated in terms of the magnetic pressure perturbation, $B_0\Delta B/4\pi$, which is in the range of 0.1 atm. It is small enough not to cause cavitation (in the regions where the pressure perturbation is negative).

The grating can be considered as a "static" grating if the laser pulse length is significantly shorter than the temporal period of the capillary waves. For lasers with pulse-width less than a fraction of microsecond, this condition is satisfied with significant margin. The driving pulse should be synchronized in such a way as to provide the maximum amplitude of the surface perturbation at the time of the arrival of the laser pulse.

5.3 Heating of conductors and of the working fluid.

The thermal conduction time over the thickness of the film, $\tau \sim h^2/2\chi$, is typically shorter than the driving pulse length. For a mercury film 5 μm thick, τ is ~10^{-5} s, less than the expected duration of the driving pulse. Assuming the worst-case scenario of one-sided cooling, from the side of the substrate, one concludes that the maximum temperature increase will occur on the surface of the film and will be determined by the relationship:

$$\Delta T = \frac{j^2 h^2}{2 c_p \chi \sigma} \equiv \frac{2\pi j^2 h^2 D_m}{c_p \chi c^2}. \tag{5.10}$$

For mercury, and the current density and other parameters as at the end of previous section, this yields a very modest temperature increase of 10^{-2} °K. On the other hand, for diffraction gratings with periods considerably shorter than 10 μm, both the current density and the temperature variation increase significantly, because of a strong dependence of the current density on the wave number. Note also that at higher values of ΔT thermal expansion of the liquid becomes substantial. This, on the one hand, may interfere with the dynamical effects discussed above but, on the other hand, may provide an alternative way for modulating the surface of the film. A more detailed analysis of all these effects is required to determine the smallest achievable period of the grating.

Consider now heating of the wires. If the width of the grating is b, and the voltage is applied at both ends of every wire, the current entering each wire from one side is $I \sim jbh/2$. Taking $j \sim 30$ kA/cm^2, $b \sim 1$mm, and $h=5$ μm, one finds that $I \sim 1$ A. For a wire made

of silver, with the resistivity of 1.62 μOhm·cm, and the thermal diffusivity ~4.53 W/cm^{0}K, the heating during the driving pulse is in the range of 10 ^{0}K.

Limitations on the intensity of the incident laser radiation are two-fold: reflective properties of the film should not deteriorate significantly during the laser pulse; mechanical perturbations created in the film by the heating of the surface layer during the pulse should not damage the substrate with embedded wires (see Sec. 3 for discussion of both issues).

5.4 Grazing incidence gratings

Grazing incidence gratings, likely to be used in x-ray optics, allow one to reduce requirements to the amplitude of the surface wave. We consider the case where the grating period λ is much longer than the wavelength λ_x of x rays,

$$\lambda_x << \lambda \tag{5.11}$$

We measure the incidence angle $\theta << 1$ from the film surface (not from the normal to the surface). One can show that, under condition (5.11), in order to have the first-order maximum shifted from the zeroth-order maximum by an angle comparable to the incidence angle and, at the same time, have a significant suppression of higher-order maximums, one has to fulfil two conditions,

$$\theta\lambda \sim 2\pi\xi, \tag{5.12}$$

and

$$2\pi\xi\theta \sim \lambda_x, \tag{5.13}$$

where ξ is the amplitude of the surface wave (see Sec. 6.2). For the given λ_x and λ these two conditions then yield the following results for the optimum incidence angle and required amplitude of surface perturbations:

$$\theta \sim \sqrt{\frac{\lambda_x}{\lambda}}, \tag{5.14}$$

and

$$\xi \sim \frac{\sqrt{\lambda\lambda_x}}{2\pi}. \tag{5.15}$$

Taking as an example $\lambda \sim 3$ μm, and $\lambda_x \sim 1.5$ Å, one finds $\theta \sim 10$ mrad, and $\xi \sim 3\cdot 10^{-7}$ cm. This amplitude, if normalized to λ, is significantly smaller than the one considered in numerical examples of Sec. 5.2. This, in turn, means that one can drive a smaller current and avoid problems with the film heating. Note that the intrinsic surface roughness evaluated in Sec. 3.3 is still much smaller than the required amplitude (5.15).

5.5 Using dielectric liquids

One can create diffraction grating based on dielectric liquids. This can be done in the same way as discussed in Sec. 4.3 in conjunction with dielectric zone plates. As dielectric liquids are generally rather poor reflectors for the normal incidence, one will have to use them in the grazing incidence mode described in the previous section. For the grating period $\lambda \sim 3$μm and the wavelength of x rays $\lambda_x \sim 1.5$ Å, the amplitude of the surface modulation, as mentioned in the previous section, should be $\xi_0 \sim 30$ Å. For a liquid with not very large dielectric constant, $\varepsilon - 1 \sim 1$, creating such perturbations would require a periodically varying electric field whose strength near the surface can be determined from the following equation:

$$\alpha\xi_0 (2\pi/\lambda)^2 \sim E^2/8\pi \tag{5.16}$$

For α~100 erg/cm^2 typical for dielectric liquids, and the other parameters as specified above, one finds that the required electric field strength is ~ 10^5 V/cm. This is beyond the breakdown field for liquid dielectrics. Therefore, one may have to resort to a resonant excitation of surface waves, as described in Sec. 6.2. This would bring the required electric field strength to a more comfortable level of 10^4 V/cm. Note that the potential difference between the wires is quite small (because of small spatial scales involved), in the range of 10V.

6. Summary

This paper describes several elements of reflecting optics based on the use of thin liquid films. The shape of the free surface of the mirrors is controlled by capillary forces and magneto-electrostatic forces (whence the acronym "CAMEL"="Capillary-Magneto-Electrostatic" introduced in Sec. 1). In the rep-rate mode, one can replace the film material in every pulse. This would allow one to keep the surface clean and initially cold even at high energy densities during each laser pulse. We have pointed out at the possibility of using planar liquid-film mirrors in the "upside-down" orientation, with the viscous inhibition of the gravitational instability. The film material will be renewed within the time short compared to the instability e-folding time. Reflecting diffraction gratings can be created by perturbing the film surface by the $\mathbf{J}\times\mathbf{B}$ force generated by an array of embedded fine wires. Gratings on the surface of dielectric liquids can be produced by electrostatic forces created by submerged conductors. Parabolic mirrors and reflecting zone plates can be created both electrostatically and electromagnetically. A focal length and the direction of the optical axis of the parabolic mirror can be changed by controlling voltages on the segmented electrodes, without any need for introducing mechanical actuators.

For rep-rate applications, an important element of the CAMEL optics is a porous substrate (perhaps, made of fused capillaries): a thin liquid layer is created over the substrate and then removed by pressing the fluid in and out through the capillaries. We have evaluated deformations of the substrate during this process. We have also discussed effect of vibrations of the mechanical structure on the distortions of the film surface and have derived conditions where vibrations are unimportant. Joule heating has been evaluated for the cases where it may be potentially important. All in all, we have presented a set of equations which could serve as a starting point for a more detailed analysis of the proposed system.

Potential applications of the CAMEL optics are numerous and include high-power lasers in various spectral ranges (from infrared to X-ray), as well as low-intensity adaptive optics systems.

Next steps in developing the CAMEL optics should include systematization of the information about possible working fluids and substrates. Among the parameters that should be screened, in addition to those listed in Table 1, there should the following ones:

1. Saturated vapor pressure over the surface.
2. Reflectivity for various wavelengths and incidence angles.
3. Cost per gram.
4. Contact angles for various substrates.
5. Products of decomposition of the film by intense laser pulse (for non-elemental working fluids).

A key issue in the experimental tests of the concept is a quality of a liquid surface produced by pressing a working fluid through the porous substrate. There is no doubt that thick-enough films with a flat surface can be produced. What has to be determined experimentally, is the *minimum* attainable film thickness (at a good surface quality). The

answer may depend on the cleanness of the substrate and its macroscopic uniformity. Direct experiments are required to address this issue.

Acknowledgment

The authors are grateful to A. Hazi, P. Springer, and J. Trebes for valuable discussion. This work was performed under the auspices of the U.S. Department of Energy by University of California Lawrence Livermore National Laboratory under contract W-7405-Eng-48, and by Stanford University, Stanford Linear Accelerator Center under contract number DE-AC03-76SF00515.

Figure captions

Fig. 1 Liquid film over solid substrate. The substrate is shaded. The surface of the film is rippled at a wavelength $\lambda \equiv 2\pi\lambda\!\!\!^{-} \equiv 2\pi/k$. Dashed line represents unperturbed surface of the film; δh s the amplitude of the surface perturbation.

Fig. 2 Dispersion properties of surface waves in the setting of Fig. 1. a) Dispersion curves for the mercury; curves, from the lower to the upper one, correspond to film thickness of 3, 30, and 100 μm, respectively; the dots show the points where the condition $\omega\tau=1$ is satisfied, where τ is defined by Eq. (2.8); dashed vertical line is the line where $k=k^*$; b) Dispersion curves for an arbitrary fluid in the dimensionless variables; curves, from the lower to the upper, correspond to the parameter k^*h equal to 10^{-1}, 10^{-2}, and 10^{-3}, respectively.

Fig. 3 Creating a thin film in the upside-down geometry: 1 – working fluid; 2 – porous substrate; 3 – liquid film; 4 – rim.

Fig.4 An example of the CAMEL-type optical system with one planar mirror oriented "upside down" and a focusing mirror having a "normal" orientation.

Fig. 5 Making a quasi-planar mirror by introducing correcting electrostatic forces. In the case shown, electric field is created between the correcting electrode 1 and the liquid mirror; 2– supporting structure (its bottom can be made of a porous material). The solid line depicts initial surface of the meniscus; the dashed line shows a corrected surface, after the voltage is applied; this surface is nearly planar near the axis.

Fig. 6 Creating a focusing mirror by introducing electrostatic field between the liquid and the ring. More sophisticated set of electrodes can be used, including electrodes segmented in the azimuthal direction.

Fig.7 Creating a mirror in a dielectric liquid. Liquid dielectric with a dielectric constant ε_1 is situated above the solid substrate with a dielectric constant ε_2. The unperturbed surface of the liquid is shown by a dashed line. After voltage is applied to a ring electrode of a radius R, the surface becomes distorted and, near the axis, acquires the shape of a focusing mirror. The second electrode is situated far from the ring.

Fig. 8 a) Creating a reflecting zone plate on the surface of a dielectric liquid by embedded circular electrodes (shown in dashed lines); the voltage is supplied via vertical conductors (thick lines); the dielectric is shown as a transparent medium; b) Creating a reflecting zone plate on the surface of a conducting liquid (transparent layer over the substrate) by driving a current between the immersed circular electrodes; the external vertical current creates an azimuthal magnetic field that allows one to keep the current between the circular electrodes at a modest level (a hole through which the vertical current crosses the zone plate is not shown). Current is supplied via vertical conductors shown in thick lines.

Fig. 9 Generating a diffracting grating on the surface of the conducting fluid by driving a current between oppositely charged wires of a planar wire array.

References

1.R.W. Moir. “Grazing incidence liquid metal mirrors (GILMM) as the final optics for laser inertial fusion power plants,” LLNL report UCRL-JC-132875 (1999).

2. P.Hickson, E.F. Borra, R. Cabana, R. Content, B.K. Gibson, G.A. Walker. “UBC/Laval 2.7 meter liquid mirror telescope,” Ap.J., v. 436, p. L201 (1994).

3.E.F. Borra, R. Content, L. Girard, S. Szapiel, L.M. Tremblay, E. Boily. “Liquid mirrors: optical shop tests and contributions to the technology,” ApJ, v. 393, p. 829 (1992).

4.R. Ragazzoni, E. Marchetti. “A liquid adaptive mirror.” Astron. Astrophys., **283**, L17 (1994).

5.R. Ragazzoni, E. Marchetti, R.U. Claudi. “Electromagnetic driven liquid mirrors.” SPIE, **2263**, 379 (1994).

6.W.L.H. Shuter, L.A. Whitehead., Astrophys. J., **424**, L139 (1994).

7.H.-E. Horng, C.-Y. Hong, S.L.Lee, C.H. Ho, S.Y. Yang, H.C. Yang. “Magnetochromatics resulted from optical gratings of magnetic fluid films subjected to perpendicular magnetic fields.” J. Appl. Phys., **88**, 5904 (2000).

8. J.V. Wehausen and E.V. Laitone. In: “*Handbuch der Physik*” (S. Flugge, Ed., Springer-Verlag, Berlin-Gottingen-Heidelberg, 1960). v. IX, Sections 15-35.

9. L.D. Landau and E.M.Lifshitz. *Fluid Mechanics* (NY, Pergamon Press, 1987). Chapter VII.

10. The LCLS Design Study Group. *Linear Coherent Light Source (LCLS) Design Study Report* , Report SLAC-R-521, Stanford University, 1998.

11. B.K. Kopbosynov, V.V. Pukhnachev. “Thermocapillary Flow in Thin Liquid Films.” Soviet Research, **15**, 95 (1986).

12. L.D. Landau and E.M.Lifshitz. *Theory of Elasticity* (NY, Pergamon Press, 1987). Chapter II.

13. A. Braslau, P.S. Pershan, G. Swislow, B.M. Ocko, and J. Als-Nielsen. “Capillary waves on the surface of simple liquids measured by x-ray reflectivity.” Phys. Rev. **A38**, 2457 (1988).

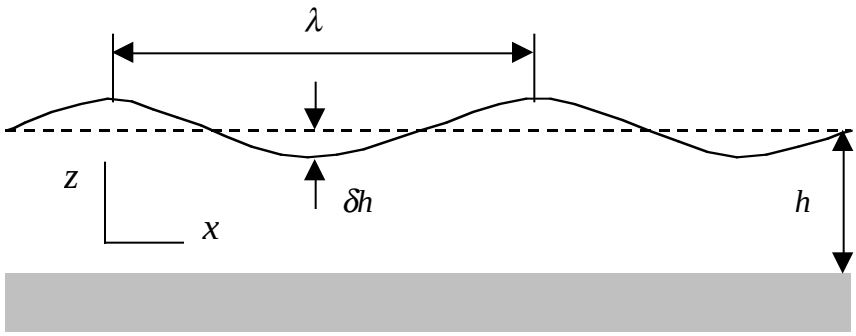

Fig.1

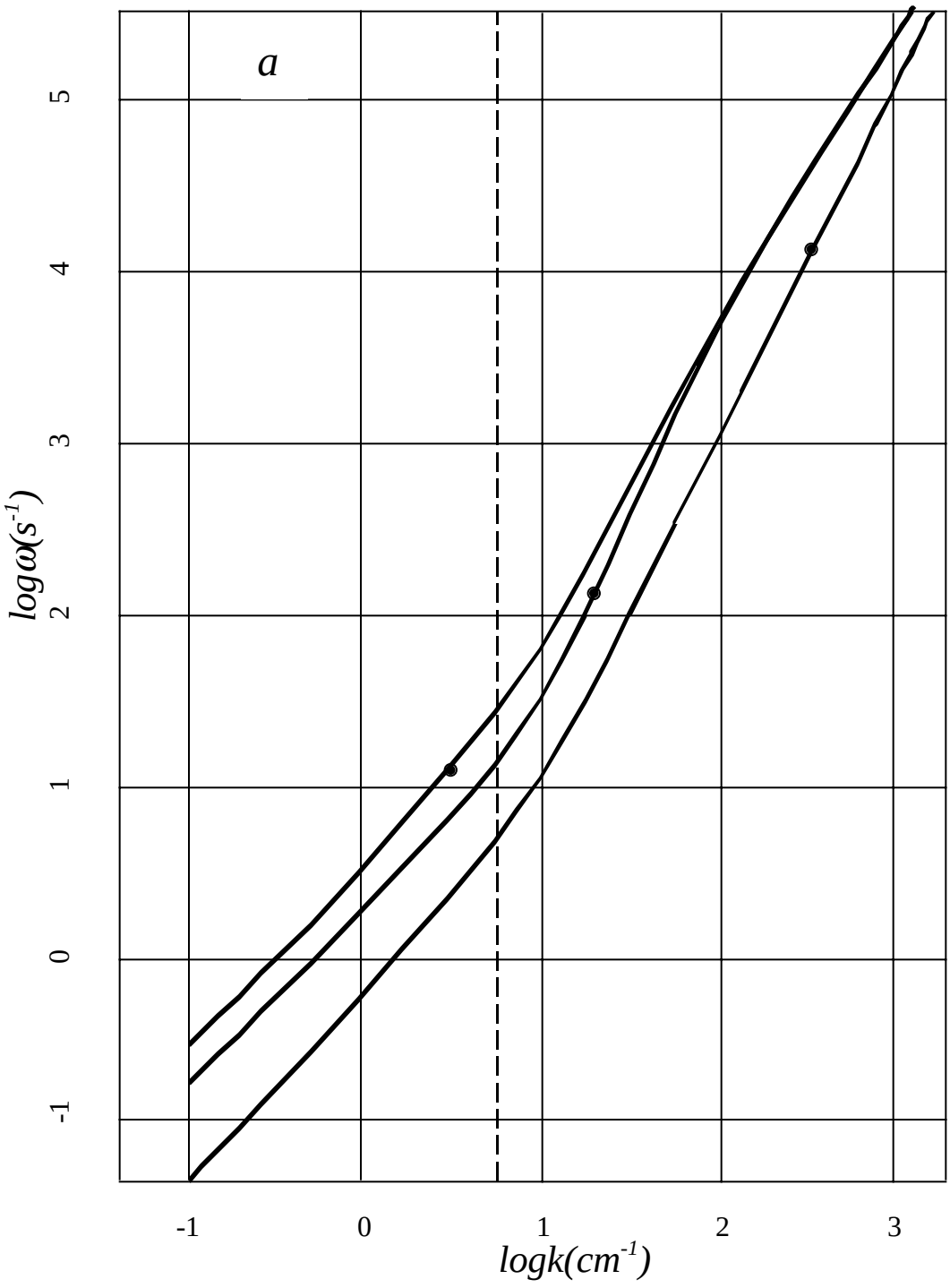

Fig.2a

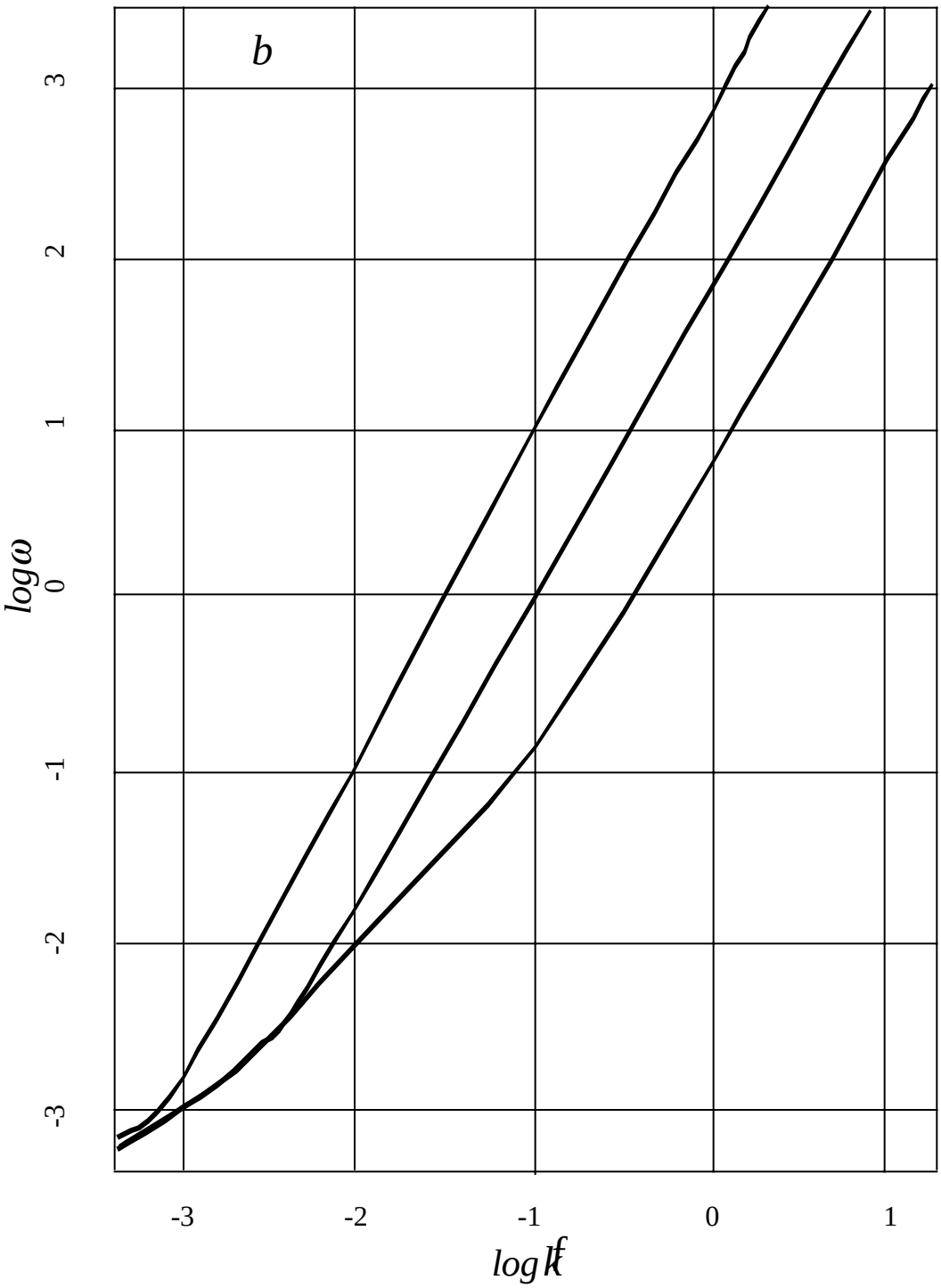

Fig.2b

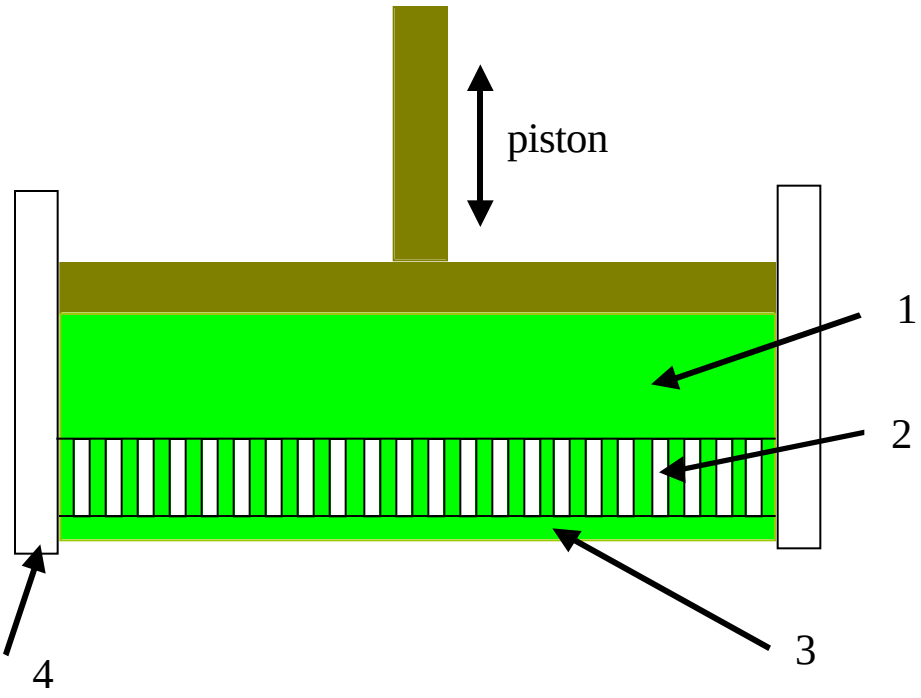

Fig.3

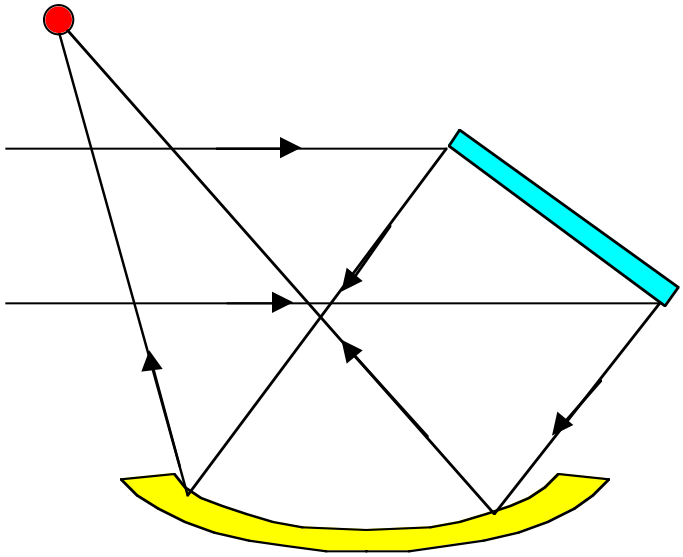

Fig.4

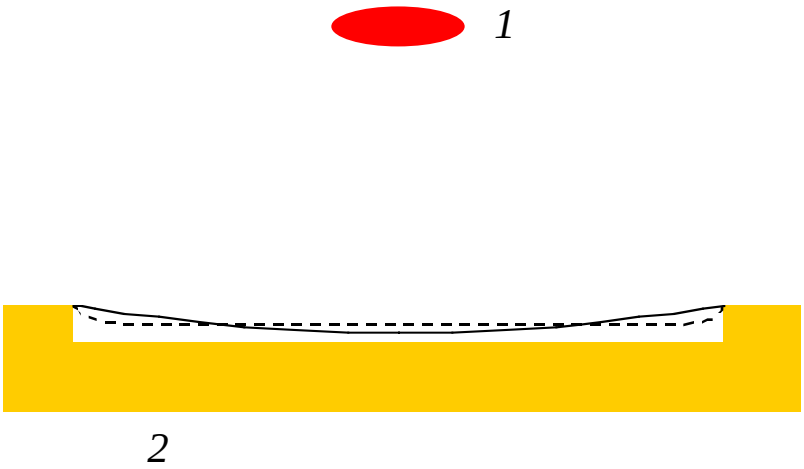

Fig.5

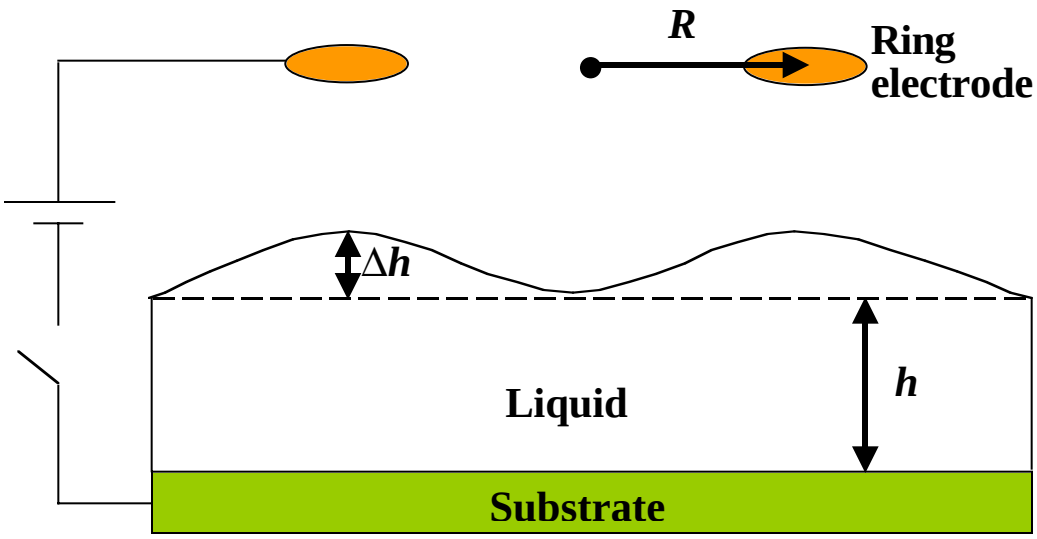

Fig.6

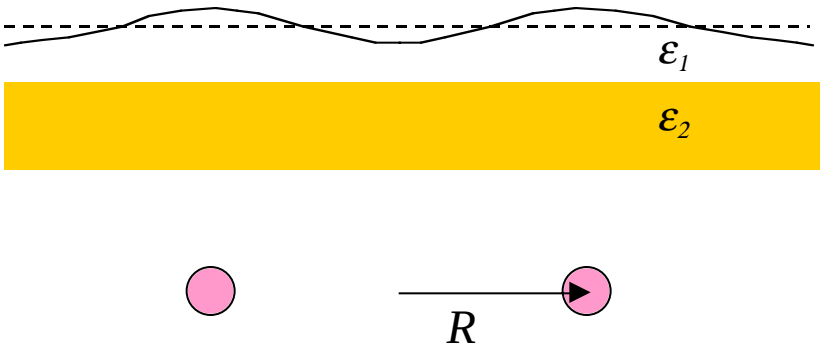

Fig.7

a

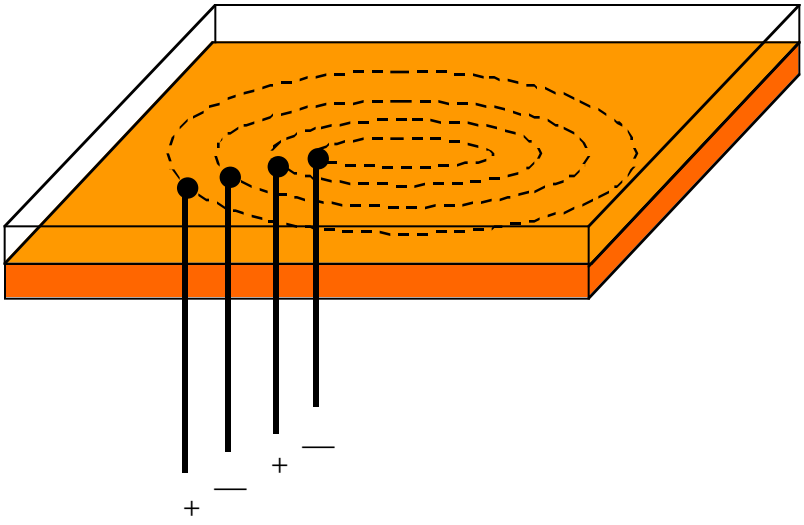

Fig.8a

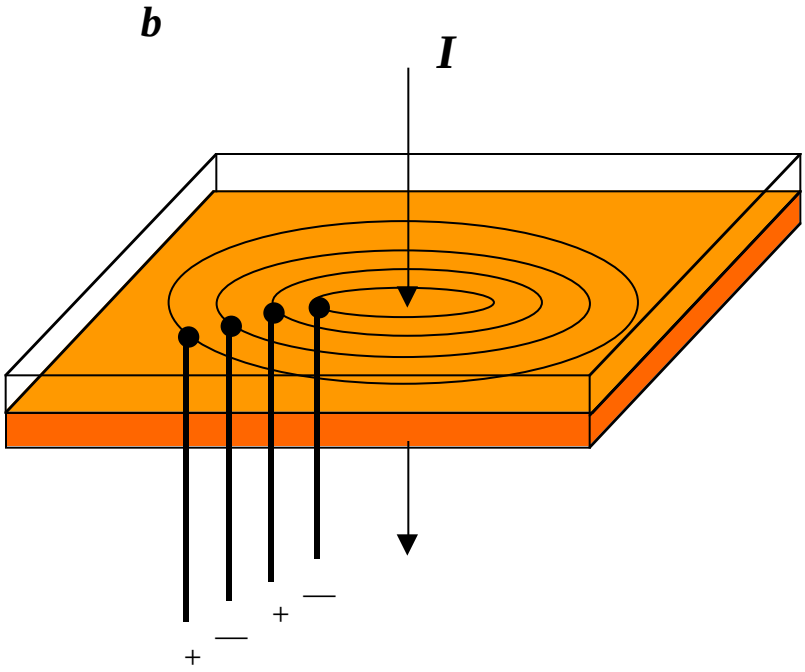

Fig.8b

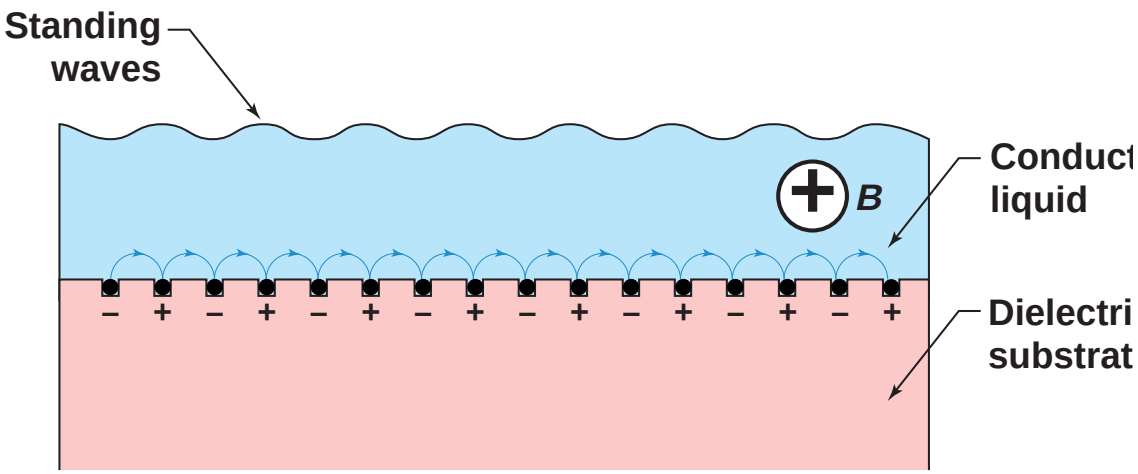

Fig. 9